Journal of Power Sources 251 (2014) 423–431

Contents lists available at ScienceDirect

Journal of Power Sources

journal homepage: www.elsevier.com/locate/jpowsour

Poly(vinylidene fluoride)/SiO_2 composite membranes prepared by electrospinning and their excellent properties for nonwoven separators for lithium-ion batteries

Feng Zhang, Xilan Ma*, Chuanbao Cao*, Jili Li, Youqi Zhu

Research Centre of Materials Science, School of Materials Science and Engineering, Beijing Institute of Technology, Beijing 100081, PR China

HIGHLIGHTS

- $PVdF/SiO_2$ composite membranes are first prepared by electrospinning.
- Inorganic silicon dioxide sol is added into blended spinning solution directly.
- Composite membranes have excellent thermal dimensional stability over a wide range of temperatures.
- Composite membranes have superior ionic conductivities.
- The electrode electrolyte interfacial resistance is low, indicating good membrane-electrode affinity.

ARTICLE INFO

Article history:
Received 26 September 2013
Received in revised form
15 November 2013
Accepted 23 November 2013
Available online 3 December 2013

Keywords:
Poly(vinylidene fluoride)
Silicon dioxide
Nonwoven separator
Electrospinning
Lithium-ion battery

ABSTRACT

$PVdF/SiO_2$ composite nonwoven membranes exhibiting high safety (thermal stability), high ionic conductivity and excellent electrochemical performances are firstly prepared by electrospinning poly(vinylidene fluoride) (PVdF) homopolymer and silicon dioxide (SiO_2) sol synchronously for the separators of lithium-ion batteries (LIBs). Differential scanning calorimetry (DSC), thermogravimetric analysis (TGA) and hot oven tests show that the $PVdF/SiO_2$ composite nonwoven membranes are thermally stable at a high temperature of 400 °C while the commercial Celgard 2400 PP membrane exhibits great shrinkage at 130 °C, indicating a superior thermal stability of $PVdF/SiO_2$ composite nonwoven membranes than that of Celgard membrane. Moreover, the composite membrane exhibits fairly high ionic conductivity (7.47×10^{-3} S cm^{-1}) that significantly improves the performance of LIBs. The $PVdF/SiO_2$ composite membranes are also evaluated to have higher level of porosity (75–85%) and electrolyte uptake (571–646 wt%), lower interfacial resistance compared to the Celgard separator. The lithium-ion cell (using $LiFePO_4$ cathode) assembled with the composite membrane exhibits more stable cycle performance, higher discharge capacity (159 mAh g^{-1}) and excellent capacity retention which proves that they are promising candidates for separators of high performance rechargeable LIBs.

1. Introduction

High-performance rechargeable lithium-ion batteries (LIBs) with long cycle life, high energy and high safety have received much attention due to the rapidly growing high energy demands [1]. In the LIB system, the anode materials and cathode materials have been widely studied as parts of a battery, however the separator is the main influence factor of safety performance of a battery, which has not drew enough attention from the public. The separator plays a vital role in preventing electronic contact between electrodes and retaining liquid electrolyte in cells [2,3]. Currently, most widely used separators in lithium-ion batteries are manufactured from polyolefins, predominantly polyethylene (PE) or polypropylene (PP) due to their suitable chemical stability, thickness, and mechanical strength [4]. However, several intrinsic factors such as low porosity, poor thermal stability, and insufficient electrolyte wettability and large difference of polarity between the highly polar liquid electrolyte and the nonpolar polyolefin separator lead to high cell resistance, low rate capability and even internal short circuits of LIBs [5–7], which severely restricts the electrochemical performance of the LIBs, especially affects the safety performance of the LIBs. Therefore, the development of new separators possessing high porosity, good thermal stability and high ionic conductivity is strongly demanded, especially in the

* Corresponding authors. Tel.: +86 10 68913792; fax: +86 10 68912001.
E-mail addresses: maxilan@bit.edu.cn (X. Ma), cbcao@bit.edu.cn (C. Cao).

0378-7753/$ – see front matter © 2013 Elsevier B.V. All rights reserved.
http://dx.doi.org/10.1016/j.jpowsour.2013.11.079

thermal stability which seriously influences the practical application of LIBs.

In this study, the fluorinated polymer poly(vinylidene fluoride) (PVdF) has been chosen as a polymer host due to its excellent thermal stability, outstanding mechanical property, inertness to solvent [4,8]. Silicon dioxide, as the second component, was adopted for the interaction between the polar group of inorganic silicon dioxide sol surface and the interaction between the polar group and fluorine atoms of PVdF molecular chain, enhanced the adhesion properties between the fibers. Moreover, the addition of inorganic silicon dioxide could decrease the crystallinity of polymer, improves absorption for the electrolyte solution and ionic conductivity, thus improve the electrochemical performance of the separator. It also could highlight the advantage of inorganic materials, thus greatly improve the heat resistance of separators, which could enhance the safety of LIBs. Eun-Sun Choi et al. have made a research about SiO_2/poly(vinylidene fluoride–hexafluoropropylene)–coated poly(ethylene terephthalate) nonwoven composite separator for a lithium-ion battery [4]. In their study, they have done much work on the influence of particle size, tunable porous structure of SiO_2 on performances of nonwoven composite separator. The separators prepared by relevant researchers provided substantial improvement in the thermal shrinkage, liquid electrolyte wettability and electrochemical performance. Nevertheless, we noted that coating modification using varisized inorganic silicon dioxide particles directly was employed, which have some problems of controlling the stability and uniformity of SiO_2 particle size during processes of preparation and charging/discharging. In view of this, in this study, silicon dioxide sol was firstly employed as a component of the blended spinning dope and it was directly spun fiber membranes dispersing in the hybrid fibers. In the prepared membranes, silicon dioxide and PVdF mixed at a molecular level, which better guaranteed the structural stability of composite membranes.

Given the low cost and ease in the construction of microstructures, nonwoven separators are especially attractive and promising to replace the conventional microporous polyolefin membranes [9,10]. In this study, electrospinning as a promising and straightforward technique that produces continuous fibers with diameter in the range of nanometers to a few microns and builds porous structure of a nonwoven for application as a separator in lithium-ion batteries was adopted. We obtained composite fiber membranes of PVdF with silicon dioxide sol using the method firstly. The prepared composite membranes have very good thermal properties, high level of porosity and electrolyte uptake in comparison with the commercial separators. The ionic conductivities of the composite membranes at ambient temperature are much higher than that for the traditional separator, Celgard 2400, saturated with $LiPF_6$ electrolyte. Moreover, the compatibility of liquid electrolyte-soaked PVdF/SiO_2 composite membranes with electrode materials was proved to be more excellent. The prepared composite membranes also exhibit good electrochemical performance for $LiFePO_4$. Furthermore, the influence of percentage composition on electrochemical performance was studied. Therefore, the composite membranes are very attractive for application to large-capacity lithium ion batteries.

2. Experimental

2.1. Preparation of composite separators

Polyvinylidene fluoride (PVdF, M_W = 400,000, Kynar 761) was purchased from Sinopharm Chemical Reagent Co., Ltd., and was vacuum dried at 60 °C for 12 h before use. N,N-Dimethylacetamide (DMAc) and acetone were purchased from Sinopharm Chemical Reagent Co., Ltd., and they were used as received without further purification.

The electrospinning method was used for the preparation of nonwoven separators. Solvent, concentration, voltage and distance are considerably important factors for the electrospinning method [11,12]. Optimized 7% PVdF solution was used for electrospinning with DMAc and acetone (3:7 weight ratio). Silicon dioxide sol is prepared by hydrolyzed tetraethoxysilane (TEOS) with ethanol (1:1 Volume ratio) at pH = 4 for 24 h. And then 7% PVdF solution and silicon dioxide sol are mixed in a certain mass ratio (9:1, 10:1) to get spinning dope which was stirred for 12 h at 60 °C. During electrospinning, the solution was fed in a 10 ml syringe and delivered with a flow rate of 2 mL h^{-1} under applied voltage of 20 kV. The distance between the needle tip and the collector was 20 cm. The electrospun fibers were accumulated on the collector, forming free-standing fibrous membranes. The resultant organic/inorganic composite membranes were then dried under vacuum at 60 °C for 12 h to remove the solvent residual before further use. Therefore, we obtained two kinds of composite membranes, one is 7% PVdF solution/silicon dioxide sol = 9:1 (wt/wt) composite membrane (hereinafter referred to as (9:1) composite membrane), another is 7% PVdF solution/silicon dioxide sol = 10:1 (wt/wt) composite membrane (hereinafter referred to as (10:1) composite membrane).

2.2. Characterization of composite separators

The morphology of the composite separators was observed by SEM. Dried composite nonwoven membranes with measured weight (W_{dry}) and volume (V_{dry}) were soaked in n-butanol (Junsei Chemical Co. Ltd.) for 2 h to obtain their wet weight (W_{wet}) after wiped from their surfaces using filter paper. The porosity of the separators was then obtained by Equation (1):

$$\text{Porosity}(\%) = \frac{W_{wet} - W_{dry}}{\rho_b V_{dry}} \times 100\% \quad (1)$$

Where ρ_b is the density of n-butanol.

The uptake of solutes in separators has an effect on the resistance of cells, and it influences the lifetime and performance of batteries [13,14]. So in this study, the electrolyte uptakes were measured in a glove box and then compared to commercial PP separator. A liquid electrolyte of 1 M $LiPF_6$ in ethylene carbonate (EC)/diethyl carbonate (DEC) = 1/1 (v/v) was employed. For the uptake measurement, weighed samples were swelled in electrolyte for 2 h and weighed again before the electrolytes were wiped using tissue paper. The electrolyte uptakes were then obtained using the increased amount of electrolyte and its Equation (2) is as follows:

$$\text{Uptake}(\%) = \frac{W - W_O}{W_O} \times 100\% \quad (2)$$

Here, W_o and W are the weights of the composite membrane before and after soaking in the liquid electrolyte, respectively.

The thermal property of the samples was measured by differential scanning calorimetry (DSC) in the temperature range of 30–210 °C at a heating rate of 10 °C min^{-1} using a TA DSC 2920. Thermogravimetric analysis (Pyris 1 TGA) was performed under air flow from 50 to 700 °C at a heating rate of 20 °C min^{-1}. The thermal shrinkage of PVdF/SiO_2 composite membranes were evaluated by measuring their (area-based) dimensional changes after they were subjected to heat treatment at various temperatures for 1 h [4,15–17].

The ionic conductivities of different separators including the Celgard membrane and electrospun PVdF/SiO_2 composite nonwoven membranes were measured by electrochemical impedance spectroscopy (EIS). The membranes were placed between two stainless steel blocking electrodes, and spectra were obtained by sweeping from 100 kHz to 0.1 Hz with an AC amplitude of 5 mV at room temperature [18]. The ionic conductivity (δ) was calculated from the following equation:

$$\delta = \frac{d}{R_b \times S} \tag{3}$$

Where R_b is the bulk resistance, and d and S are the thickness and area of the fibrous membrane, respectively.

The interfacial resistances between liquid electrolyte-soaked PVdF/SiO_2 composite fibrous membranes and electrodes were evaluated by electrochemical impedance spectroscopy (EIS). During the measurements, the liquid electrolyte soaked separators were sandwiched between $LiFePO_4$ (Raw materials were purchased from China Titans Energy Technology Group Co., Ltd.) cathode materials and lithium metal anode materials. The measurements were carried out at an amplitude of 5 mV over a frequency range of 100 kHz to 0.1 Hz using an electrochemical analyzer CHI 660D (Shanghai Chenhua Instrument Inc. China). Prior to the measurements, all test units rested at room temperature for 24 h.

For evaluation of electrochemical performance for the cells with various separators, a coin-type cell (CR2025) was used in half-cell configuration assembled in a configuration of $LiFePO_4$/separator/lithium metal. The charge and discharge cycling tests of the lithium-ion cells were conducted using the LAND battery cycle system (Wuhan Blue Electric Co., LTD, China) over a voltage range of 2.0–4.2 V at a constant charge current of 0.2C rate.

3. Results and discussion

3.1. Morphologies and porosities

Two PVdF/SiO_2 composite nonwoven membranes with different PVdF solution and SiO_2 sol ratios (9:1 and 10:1, wt/wt) prepared by electrospinning consist of multi-fibrous layers with a number of interstices/pores between the fibers. The morphologies were observed on SEM images (Fig. 1). The images showed that the composite fibers formed and its pore structures were totally built. Elemental analysis spectrograms (Fig. 2) corresponding to Fig. 1 show silicon dioxide inorganic components have been added to composite nonwoven membranes successfully. TEM images (Fig. 3) of two composite membranes which show distribution of SiO_2 particles in fibers, further confirm the formation of the composite membranes. It can be seen that some particles adhere to the surface of fibers, some particles may enter the fibers. It could be supposed that the porous composite separators were prepared well. From the typical image of the electrospun composite fibers, it can be found that the PVdF/SiO_2 composite fibers are randomly oriented. The membrane of the composite fibers exhibits a three-dimensional porous network structure. Fiber diameter distribution of composite membranes are shown in Fig. 4. Obviously, the diameter of most fibers ranges from 150 nm to 280 nm. Moreover, the fiber diameter of (9:1) composite membrane which exhibits better pore interconnectivity is more uniform than that of (10:1) composite membrane. The average pore size of (9:1) composite membrane is smaller than that of

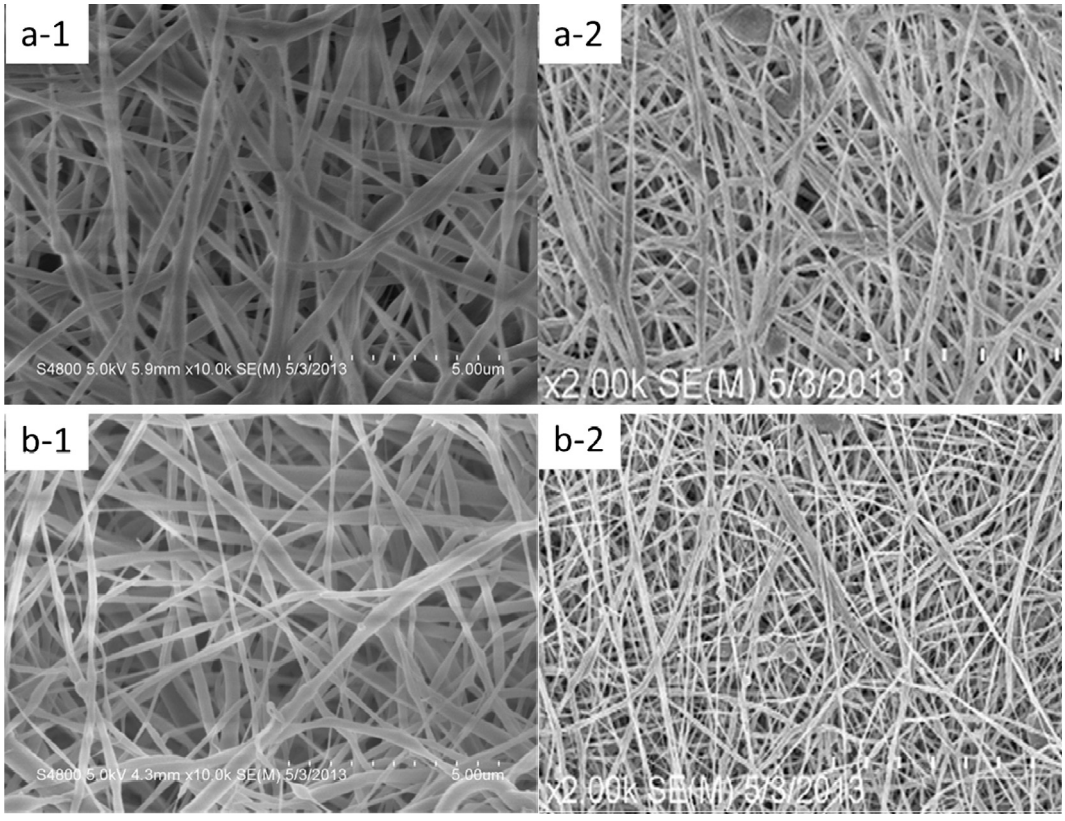

Fig. 1. SEM images at high and low magnifications for (9:1) (a) and (10:1) (b) composite membranes.

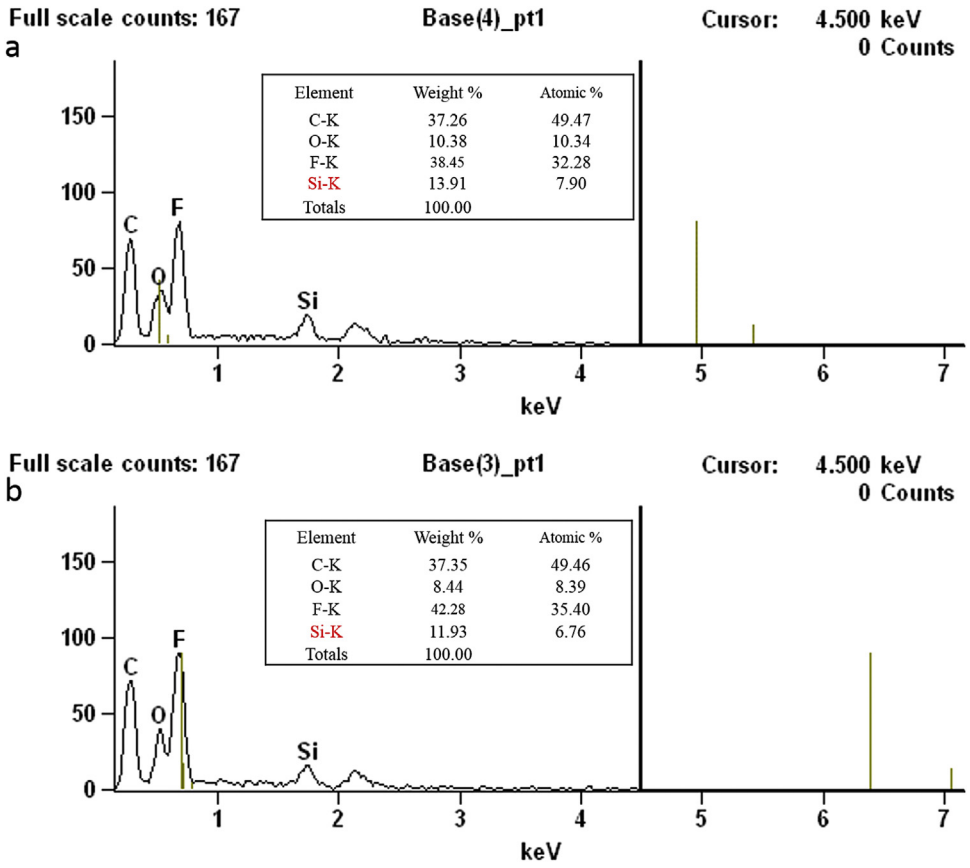

Fig. 2. Elemental analysis spectrograms of (9:1) (a) and (10:1) (b) composite membranes.

(10:1) composite membrane (Fig. 5). More pores with smaller size provide more channels for lithium ion, accelerate mobility of lithium-ion. Furthermore, cross-section SEM (Fig. 6) of composite membranes are consistent with Fig. 1, which not only show the morphology of fibers, but also confirm the three-dimensional network structure of composite membranes. Besides, it can also be seen that the surface of PVdF/SiO_2 composite fibers is smooth. To some extent, it can be see that the specific separator with suitable pore size and porosity for the application in a secondary battery was successfully prepared.

From Table 1, it can be seen that the PVdF/SiO_2 composite separators have higher porosities and better uptakes for the electrolyte than that of the Celgard separator. This is closely related to the preparation method – the electrospinning method that is more inclined to obtain nonwoven membrane with higher porosity. Compared to Celgard 2400 PP membrane, PVdF is a polar polymer,

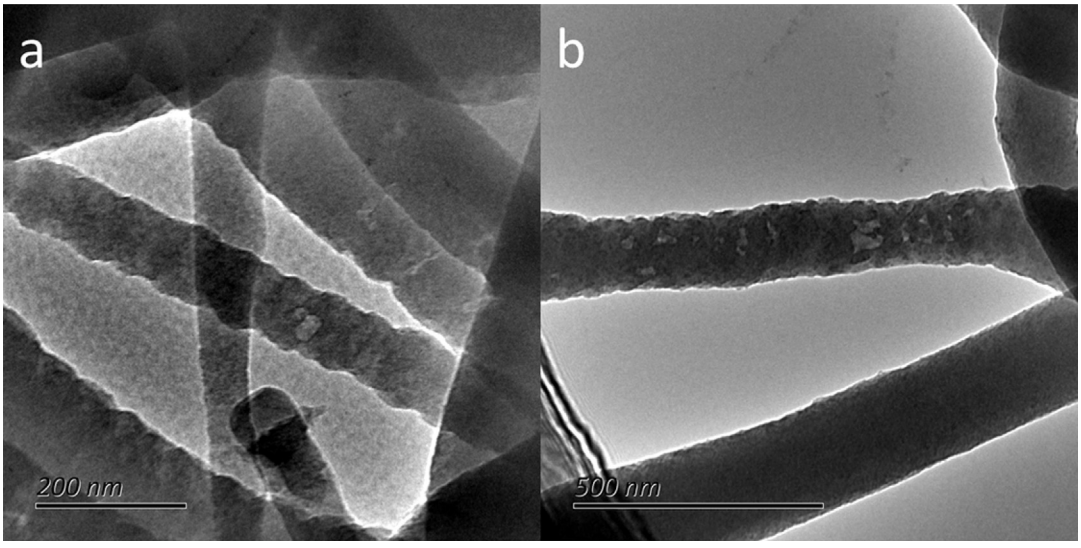

Fig. 3. TEM images of (9:1) (a) and (10:1) (b) composite membranes.

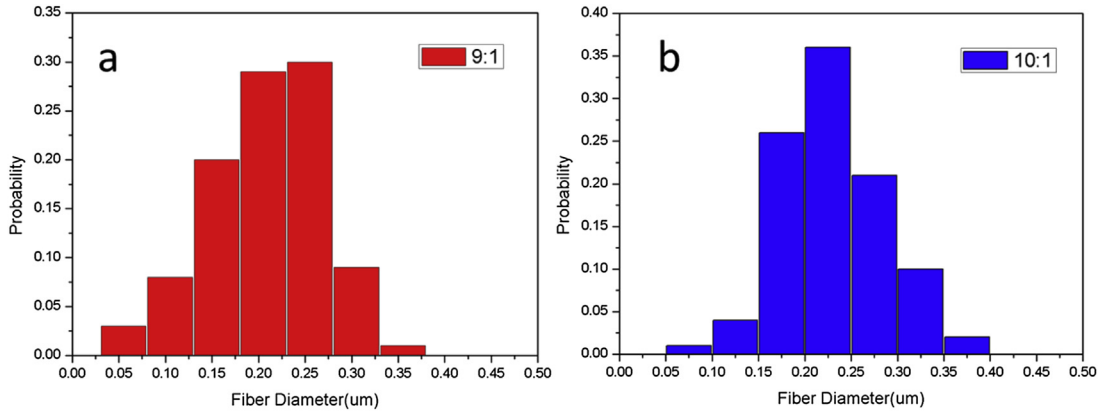

Fig. 4. Fiber diameter distribution histograms of (9:1) (a) and (10:1) (b) composite membranes.

it is easier to absorb more organic electrolyte solution. Besides, the full interconnectivity of micropores and the existence of silicon dioxide inorganic components also contribute to more outstanding absorption of the electrolyte.

3.2. Thermal properties

In order to investigate thermal stabilities of separators, the thermal stability of the separators was first evaluated by DSC (Fig. 7a). The Celgard 2400 PP membrane separator shows endothermic peaks at 132 °C and 158.5 °C. This is probably because the molecular chains of Celgard 2400 PP membrane were one-way stretched in the process of machining, which could lead to orientation induced crystallization. When heated to the temperature of 132 °C, the crystallization of Celgard 2400 PP membrane decreased with curliness of molecular chain, resulting in macro performance shrink, which is a serious safety risk for lithium-ion batteries. Whereas, no endothermic peaks can be observed up to 161 °C for the PVdF/SiO_2 composite membranes, which indicates that the thermal stability of PVdF/SiO_2 composite membrane is much better than that of Celgard. TGA was also carried out to explore the thermal properties of the separators (Fig. 7b). It can be seen that the onset temperatures of severe degradation (Tonset) of PVdF/SiO_2 composite membranes are roughly same to that of Celgard PP membrane at about 400 °C, even though the composite membranes had a very small amount of degradation when heated up to 400 °C which may be due to volatilization of the residual solvents. But, when heated to 480 °C, Celgard PP membrane degraded completely, which severely reduces the safety of LIBs. As a comparison, when heated to 500 °C, there are still more than 30% of the composite membranes after degradation. More notably, the remaining amounts of the composite membranes are still more than 25% until heated to 700 °C, further demonstrating the superior thermal stability of PVdF/SiO_2 composite membranes. The results show that the composite membranes significantly improved the safety of LIBs. These are not just because of PVdF skeleton material, and it is due to inherent heat resistance of inorganic silicon dioxide component which strengthened the overall frame of heat resistance.

To characterize thermal dimensional stability of membranes, Fig. 8a shows that Celgard 2400 PP membrane and PVdF/SiO_2 composite membrane were treated in an oven for 1 h at 80, 100, 110, 120, 130, 140, 150 and 160 °C, respectively. The result is also shown in Fig. 8. It is observed that Celgard 2400 PP shows serious shrinkage after thermal treatment at 120 °C and it continues to thermally shrink with increasing temperature. By contrast, the (area-based) dimensional change of PVdF/SiO_2 composite membrane is negligible over a wide range of temperatures which owe to addition of inorganic silicon dioxide, which greatly improves the heat resistance of polymer materials. The difference in the thermal shrinkage between the PP separator and PVdF/SiO_2 composite membrane becomes more pronounced as the temperature is increased to 130 °C. Fig. 3b presents photographs of the separators after being exposed to 130 °C and 150 °C for 1 h. It can be seen that the Celgard membrane exhibits great shrinkage with the color change from white to transparent as it experienced stretching processes. While for the PVdF/SiO_2 composite membranes no color change and shrinkages are observed after the hot oven tests, which

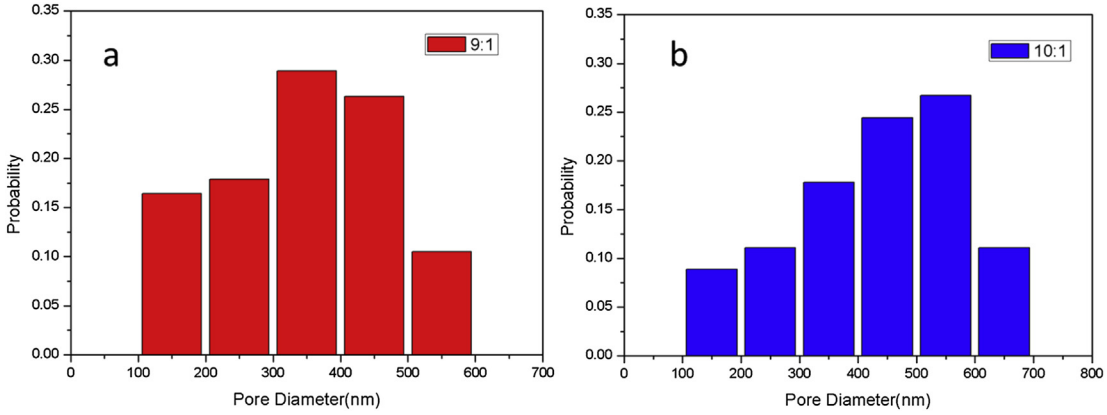

Fig. 5. Pore size distribution histograms of (9:1) (a) and (10:1) (b) composite membranes.

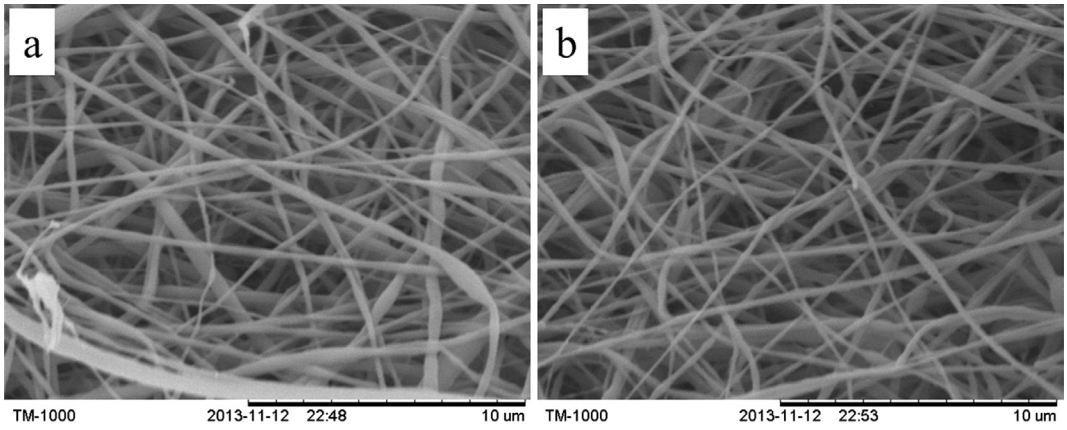

Fig. 6. Cross-sectional SEM of (9:1) (a) and (10:1) (b) composite membranes.

Table 1
Porosities and uptakes of different separators.

Properties	PP	7% PVDF solution/SiO_2 sol (wt/wt)	
		9:1	10:1
Thickness (μm)	25	83	85
Porosity (%)	30	85	75
Uptake (%)	233	646	571

suggest that the internal structure of composite membranes, especially the crystallinity does not take place obvious changes. All these results show that the addition of inorganic silicon dioxide successfully improved the heat resistance of the separators, improved the safety of the lithium ion batteries. Thus, it can be expected that the thermal stability of the lithium ion batteries will be significantly improved when PVdF/SiO_2 composite nonwovens are applied as lithium ion battery separators.

3.3. Ionic conductivities

Fig. 9 shows the Nyquist curves of the liquid electrolyte-soaked PVdF/SiO_2 fibrous membranes. The conductivity can be obtained from the high-frequency intercept of the Nyquist curve on the z'-axis, from which the ionic conductivity was determined according to Equation (3). Thus, the ionic conductivities of the (9:1), (10:1) PVdF/SiO_2 electrolytic membranes can be calculated to be 7.47×10^{-3} S cm^{-1}, 3.49×10^{-3} S cm^{-1} at room temperature. The high porosities of the electrospun PVdF/SiO_2 composite separators and full interconnectivity of macropores make the ions migrate easily, resulting in high ionic conductivities at room temperature. For comparison, the ionic conductivity of the Celgard electrolytic membrane is 4.1×10^{-5} S cm^{-1}. Therefore, the ionic conductivities of liquid electrolyte-soaked PVdF/SiO_2 membranes are far superior to that of Celgard 2400 PP membrane. The results show that the good pore interconnectivity and high porosity could improve the ionic conductivity of the electrospun PVdF/SiO_2 composite membrane. In addition, it is assumed that the existence of silicon dioxide inorganic components is helpful to increase of ionic conductivity. Since the ionic conductivity depends on the mobility of electrolytic solution, the increased electrolyte uptake may well increase the ionic conductivity. The higher porosity and better uptake of PVdF/SiO_2 composite nonwovens than those of Celgard membrane are beneficial for the infiltration of the separators by the liquid electrolyte, which facilitates the migration of lithium ions in the composite membranes, thus resulting in the lower resistance of PVdF/SiO_2 composite membranes and promoting the penetration of the electrolyte and the migration of lithium ions for better battery performance.

3.4. Interfacial resistance

The compatibility of liquid electrolyte-soaked PVdF/SiO_2 composite membranes with electrode materials was investigated by measuring electrochemical impedance spectra (EIS) of $LiFePO_4$/liquid electrolyte soaked membrane/Li cells and the results are

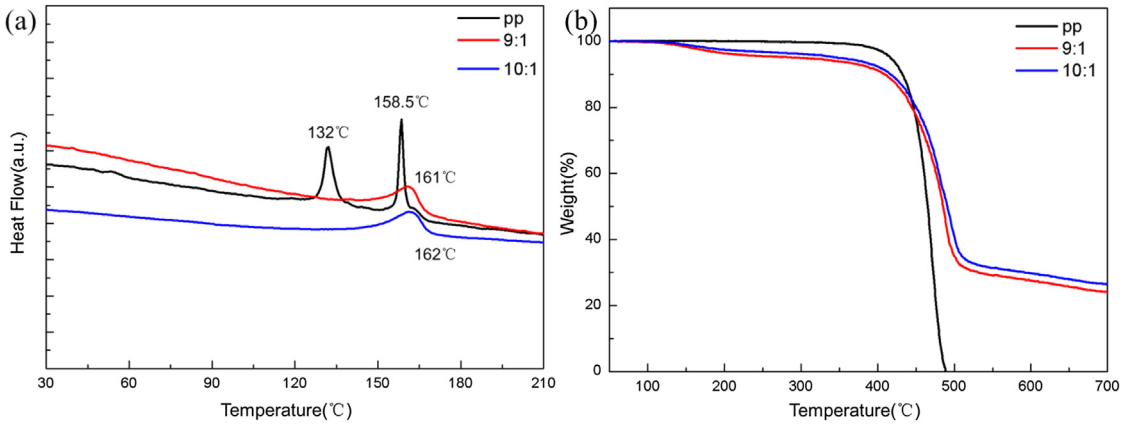

Fig. 7. (a) DSC and (b) TGA curves of Celgard PP membrane (9:1) and (10:1) composite membranes.

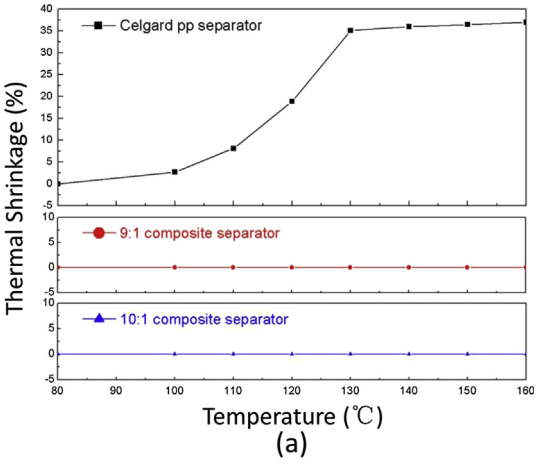

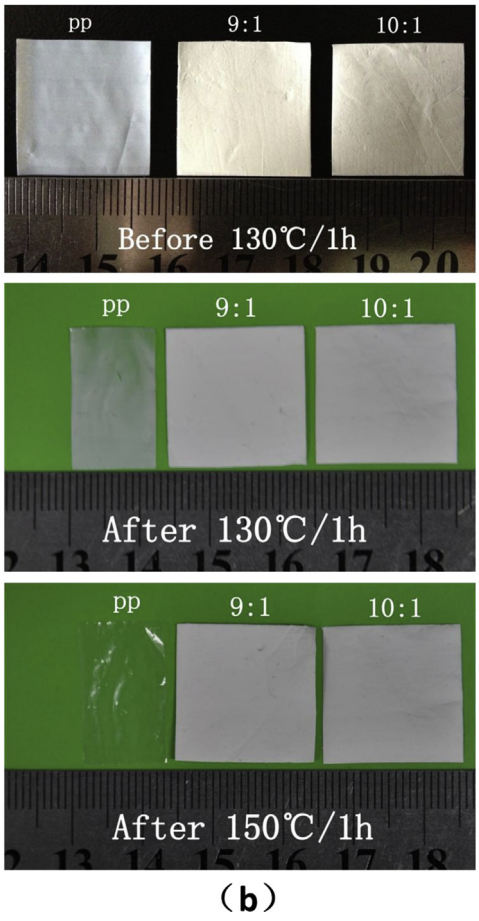

Fig. 8. (a) Thermal shrinkage of PP separator and PVdF/SiO_2 composite membranes as a function of heat-treatment temperature. (b) Photographs of the separators after exposure to 130 °C and 150 °C for 1 h.

shown in Fig. 10. In this EIS curve, the left intercept on the Z′-axis of the intermediate-frequency semicircle represents the bulk resistance (R_b) while the diameter of the semicircle indicates the electrode–electrolyte interfacial resistance (R_{in}). As shown in Fig. 10, the order of R_{in} values is: (9:1) composite membrane (86Ω) ≈ (10:1) composite membrane (85Ω) < Celgard 2400 PP membrane (123Ω). Both the (9:1) composite membrane and (10:1) composite membrane show lower interfacial resistances than that of commercial Celgard 2400 PP membrane, which is due to their large porosities and high electrolyte uptakes, as well as the good

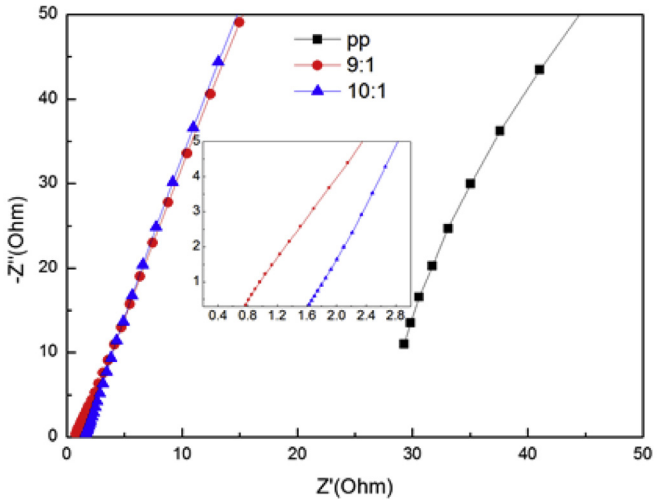

Fig. 9. Ionic conductivities of liquid electrolyte-soaked PVdF/SiO_2 composite membranes.

membrane-electrode affinity [19,20], which facilitates the migration of lithium ions at the electrode/electrolyte interface and leads to a decrease in the cell resistance.

3.5. Electrochemical performances

Fig. 11 shows the initial charge–discharge curves at the 0.2C (1C = 170 mA g^{-1}) rate for the cells using the Celgard 2400 PP separators and PVdF/SiO_2 composite fibrous membranes as separators. All the curves show stable charge and discharge plateaus with discharge capacities of 142, 151 and 159 mAh g^{-1} for the Celgard 2400 PP separators, (9:1) and (10:1) composite fibrous membranes respectively. Due to the smaller diameter, higher porosity and better uptake for the electrolyte, the capacities of PVdF/SiO_2 composite fibrous membranes are higher than that of the Celgard membrane separator.

The cell performances of the composite separators, which include discharge capacity, discharge C-rate capability, and cyclability at a charge/discharge condition of 0.2C rate were investigated. Fig. 12 depicts the discharge profiles of cells, wherein the cells were

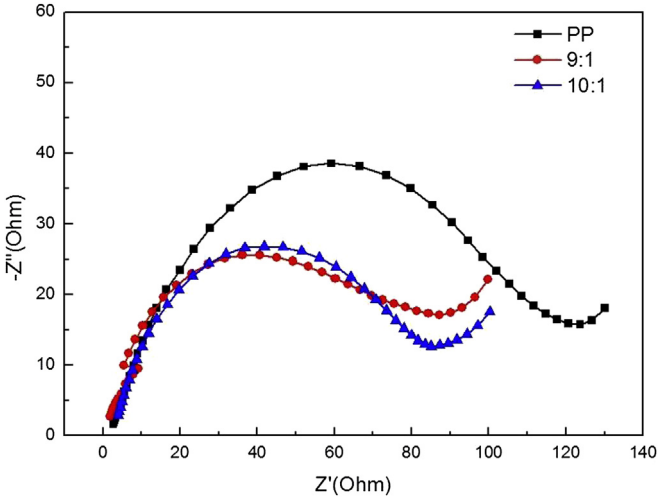

Fig. 10. Nyquist plots for the cells with Celgard PP membrane, (9:1) and (10:1) composite membranes as separators, respectively.

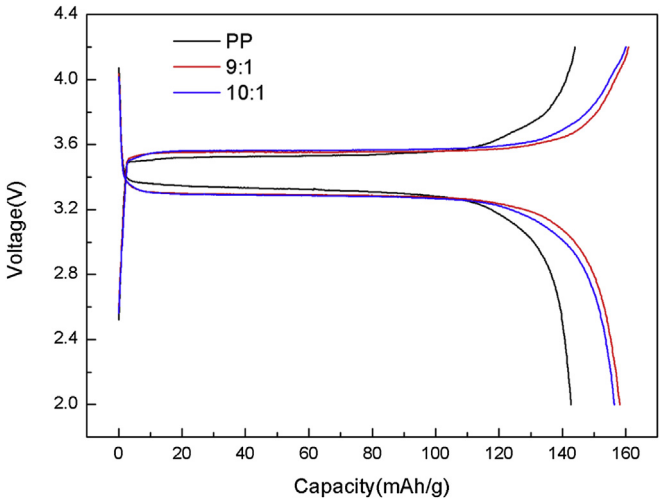

Fig. 11. Initial charge–discharge curves for the cells using Celgard membrane, (9:1) and (10:1) composite membranes as separators, respectively.

charged under a voltage range between 2.0 and 4.2 V at a constant charge current density of 0.2C and discharged at various current densities ranging from 0.2 to 1.0C. A notable finding is that the (9:1) composite separator presents higher discharge capacities than that of the (10:1) composite separator and that of the pristine PP separator over a wide range of discharge current densities. This difference in the discharge capacities between the composite separators suggests that the silicon dioxide component content has a certain influence on electrochemical performance of LIBs.

This interesting discharge C-rate capability behavior can be further discussed by considering the ionic conductivity of separators. Table 2 shows that the (9:1) composite separator has higher ionic conductivity (7.47×10^{-3} S cm^{-1}), as compared to the (10:1) composite separator (3.49×10^{-3} S cm^{-1}) and Celgard PP separator (4.1×10^{-5} S cm^{-1}). The previous results on the morphology (Fig. 1) and the porosity (Table 1) verify that a more porous structure is developed in the (9:1) composite separator, possibly yielding a shorter tortuous path for ion movement. In addition, the (9:1) composite separator shows larger electrolyte uptake (Table 1). Both the highly-developed porous structure and good electrolyte uptake are expected to allow more facile ion transport in the (9:1)

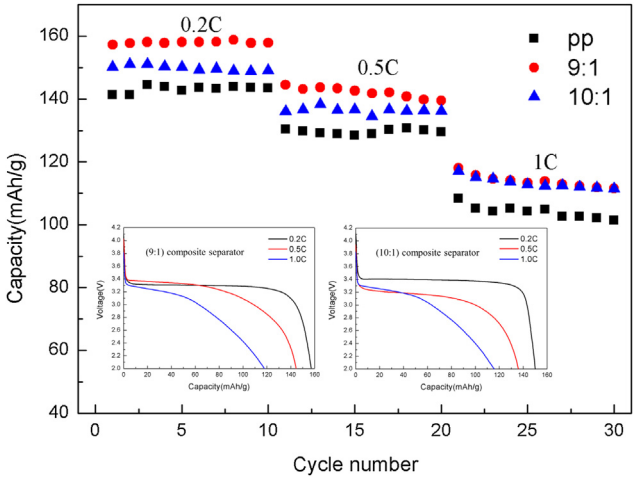

Fig. 12. Results of rate capability tests for the cells with Celgard PP membrane and composite nonwoven separators.

Table 2
Ionic conductivities of different separators.

Property	PP	7% PVDF solution/SiO_2 sol (wt/wt)	
		9:1	10:1
Ionic conductivity (S cm^{-1})	4.1×10^{-5}	7.47×10^{-3}	3.49×10^{-3}

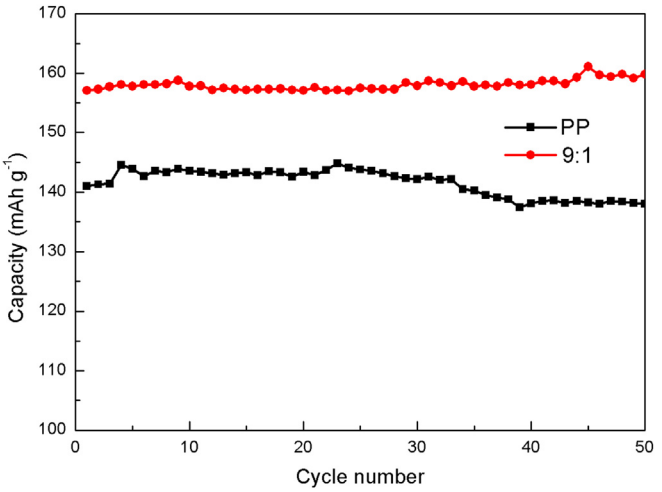

Fig. 13. Cycle performance for the cell with Celgard PP membrane and (9:1) composite nonwoven separator at 0.2C rate.

composite separator, which thus contributes to improving the discharge C-rate capability of the cells. In comparison, for the (10:1) composite separator, sluggish ion transport due to the low porosity and small electrolyte uptake may be responsible for the relatively low discharge C-rate capability.

The cycle performance (i.e., the discharge capacity of cells as a function of cycle number) of composite separators was investigated, wherein the cells were cycled between 2.0 and 4.2 V at constant charge/discharge current density (0.2C/0.2C). Fig. 13 shows that the (9:1) composite separator delivers excellent discharge capacity up to the 50th cycle (159 mAh g^{-1}, capacity retention is close to 100%), as compared to the Celgard 2400 PP separator (136 mAh g^{-1}, capacity retention is less than 95%). Every cycle of charge/discharge is very steady (efficiency is close to 100%, Fig. 14). The remarkable improvement in the cyclability of the (9:1)

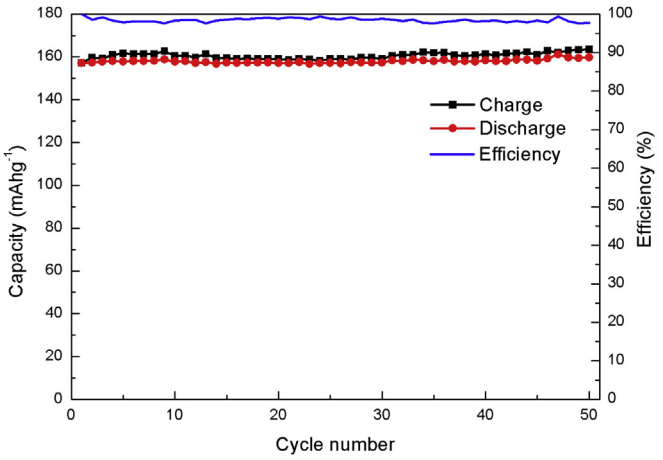

Fig. 14. Charge–discharge curves and efficiency for the cell with (9:1) composite nonwoven separator at 0.2C rate.

composite separator may be attributed to its highly porous structure (Fig. 1) as well as strong affinity for the liquid electrolyte (Fig. 9), as these factors could impart more facile ion transport and better electrolyte retention during the cycling process.

4. Conclusions

PVdF/SiO_2 organic/inorganic composite nonwoven membranes with formula proportion have been successfully fabricated via electrospinning for the separators of LIBs. The prepared composite separators showed high level of porosity (75–85%) and electrolyte uptake (571–646 wt%) in comparison to Celgard PP separator. What is more important is that PVdF/SiO_2 composite separators provided substantial improvement in the thermal shrinkage, due to the presence of heat-resistant PVdF nonwoven supports and inorganic silicon dioxide constituents, which greatly improved the safety of LIBs. In comparison to the (10:1) composite separator, the (9:1) composite separator offered a highly-developed porous structure (i.e., higher porosity, shorter tortuous path and more full interconnectivity of macropores) and larger electrolyte uptake per unit volume of a separator, which contributed to the higher ionic conductivity. This facile ion transport, in conjunction with lower interfacial resistance, played a crucial role in the improved cell performance of the (9:1) composite separator. In cell test, at 0.2C rate, Li/$LiFePO_4$ cells using the PVdF/SiO_2 composite membranes as separators gave an excellent performance in first-cycle charge/discharge capacities (159, 156 mAh g^{-1}) and stable cycle performance, and it exhibited high efficiency of each charge/discharge and very good capacity retention as compared to the Celgard 2400 PP separator. Furthermore, the preparation process of the composite membranes is very simple. Therefore, PVdF/SiO_2 composite separators are promising candidates for separators of high-performance rechargeable lithium-ion batteries.

Acknowledgment

This work was supported by National Natural Science Foundation of China (Grants 21371023).

References

[1] Y.-G. Guo, J.-S. Hu, L.-J. Wan, Adv. Mater. 20 (2008) 2878–2887.
[2] Y. Liang, L. Ji, B. Guo, Z. Lin, J. Power Sources 196 (2011) 436–441.
[3] D. Bansal, B. Meyer, M. Salomon, J. Power Sources 178 (2008) 848–851.
[4] E.-S. Choi, S.-Y. Lee, J. Mater. Chem. 21 (2011) 14747.
[5] T.H. Cho, T. Sakai, S. Tanase, K. Kimura, Electrochem. Solid-State Lett. 10 (2007) A159–A162.
[6] S.S. Zhang, J. Power Sources 164 (2007) 351–364.
[7] Y.M. Lee, J.-W. Kim, N.-S. Choi, J. Power Sources 139 (2005) 235–241.
[8] K. Hwang, B. Kwon, H. Byun, J. Membr. Sci. 378 (2011) 111–116.
[9] D.-J. Yang, I. Kamienchick, D.Y. Youn, Adv. Funct. Mater. 20 (2010) 4258–4264.
[10] Y. Zhu, F. Wang, L. Liu, Energy Environ. Sci. 6 (2013) 618.
[11] F. Croce, M.L. Focarete, J. Hassoun, Energy Environ. Sci. 4 (2011) 921–927.
[12] B. Scrosati, Nature 373 (1995) 557.
[13] W.H. Seol, Y.M. Lee, J.K. Park, J. Power Sources 163 (2006) 247.
[14] R.B. MacMullin, G.A. Muccini, J. AIChE 2 (1956) 393–403.
[15] H.S. Jeong, J.H. Kim, S.Y. Lee, J. Mater. Chem. 20 (2010) 9180.
[16] J.H. Park, J.H. Cho, W. Park, D. Ryoo, S.J. Yoon, J.H. Kim, Y.U. Jeong, S.Y. Lee, J. Power Sources 195 (2010) 8306.
[17] H.S. Jeong, S.C. Hong, S.Y. Lee, J. Membr. Sci. 364 (2010) 177.
[18] Y.Z. Liang, S.C. Cheng, J.M. Zhao, J. Power Sources 240 (2013) 204–211.
[19] P. Raghavan, X.H. Zhao, J. Manuel, C. Shin, M.Y. Heo, J.H. Ahn, Mater. Res. Bull. 45 (2010) 362–366.
[20] H.R. Jung, D.H. Ju, W.J. Lee, X.W. Zhang, R. Kotek, Electrochim. Acta 54 (2009) 3630–3637.